Slip Line Growth as a Critical Phenomenon

Fabio Leoni
Dipartimento di Fisica, Sapienza Università di Roma, Piazzale Aldo Moro 2, 00185 Roma, Italy

Stefano Zapperi
CNR-INFM, S3, Dipartimento di Fisica, Università di Modena e Reggio Emilia, via Campi 213/A, I-41100, Modena, Italy
ISI Foundation, Viale San Severo 65, 10133 Torino, Italy
(Received 1 December 2008; published 18 March 2009)

We study the growth of a slip line in a plastically deforming crystal by numerical simulation of a double-ended pileup model with a dislocation source at one end, and an absorbing wall at the other end. In the presence of defects, the pileup undergoes a continuous nonequilibrium phase transition as a function of stress, which can be characterized by finite-size scaling. We obtain a complete set of critical exponents and scaling functions that describe the spatiotemporal dynamics of the slip line. Our findings allow us to reinterpret earlier experiments on slip line kinematography as evidence of a dynamic critical phenomenon.

DOI: 10.1103/PhysRevLett.102.115502 PACS numbers: 61.72.Lk, 68.35.Rh, 81.40.Lm

Plastic deformation in crystals is due to the motion of dislocations driven by the external stress. In recent years, experimental and theoretical work has shown that dislocation dynamics is a complex intermittent phenomenon involving the collective motion of many interacting dislocations [1]. In particular, a deformation test on micron-scale crystals has revealed intriguing size effects and power-law distributed strain bursts [2,3], which have been reproduced in dislocation dynamics simulations [4]. Intermittent dislocation motion is a generic feature of plasticity, not only in micron-scale samples, as shown recently by acoustic emission measurements [5,6] and by earlier reports from slip line kinematography in macroscopic samples [7–9]. These experimental observations lead to the idea that plastic yielding is a nonequilibrium critical point [1], similar to the jamming transition observed in soft and glassy materials [10] or the depinning transition for disordered elastic manifolds [11].

The yielding transition has been investigated in various dislocation models, from the dynamics of an individual flexible dislocation interacting with quenched random impurities such as solute atoms [12,13] to the dynamics of several rigid dislocations moving on single slip systems [14,15]. While these models provided a good understanding of the yielding transition in simplified conditions, less is known about the role of dislocation nucleation and multiplication for the critical behavior. In very clean single crystals, with a very small initial dislocation density, dislocations are most likely nucleated from sources present at the surface of the sample, where it is easy to find defects (steps, scratches) acting as stress concentrators. In this case, the onset of plasticity corresponds to the creation and propagation of slip lines through the entire cross section of the crystal.

A slip line can be envisaged as a queue of dislocations, a pileup, pushed through a series of obstacles, such as solute atoms or immobile dislocations from other glide planes (see Fig. 1). Experimentally slip lines can terminate or propagate depending on the value of the shear stress, temperature, crystal structure, and types of defects [16]. A transition from homogeneous to inhomogeneous slip, with increasing impurity concentration, is observed experimentally in fcc alloys [17,18]. Here, we investigate the dynamics of a double-ended pileup in the presence of defects, with a source of dislocations at one end and an absorbing wall at the other. In the present model, the stress dependence of the stationary dislocation density, velocity, and strain rate obey finite-size scaling. This result indicates

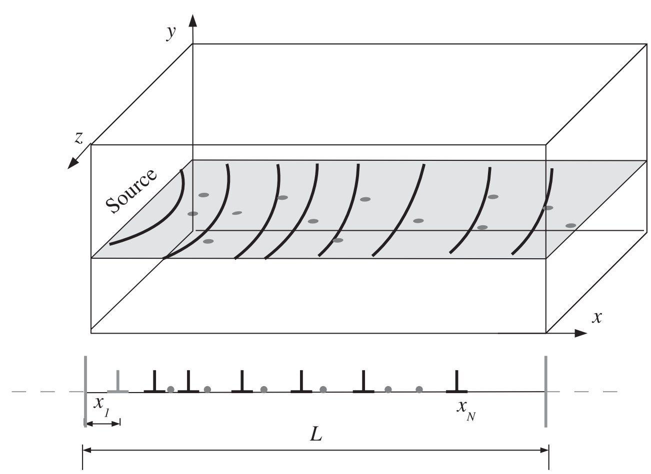

FIG. 1. At the top, we show a three dimensional sketch of a slip plane line containing a pileup of dislocations emitted by a source placed on the left surface and absorbed at the right-hand side of the sample. Our simplified model is shown in the bottom part of the figure: dislocations move on a line of length L and interact with each other, with image dislocations and with point impurities. The source is modeled as an immobile dislocation with varying Burgers vector placed at x_1.

that the transition observed in earlier experiments should be reinterpreted as a signature of a continuous nonequilibrium critical phenomenon. The scaling exponents we measure in the present model are different from those found in the corresponding homogeneous system, where nucleation is not considered and the dislocation density is constant [19]. On the other hand, the present model accounts for disorder and more realistic dislocation sources with respect to the model described in Ref. [14].

We consider the pileup as a group of identical edge or screw straight dislocations parallel to the z axis that can move in the positive x direction in the plane $y = 0$ when the net force acting on them is positive. This corresponds to an effective one-dimensional model in which the dislocations are generated from a source in the left side of a line of length L (see Fig. 1). They interact with each other and with a disordered stress landscape provided by solute atoms, or other defects, and disappear when they reach the right side of the line. The dislocations have coordinates x_i, with $i = 1, \ldots, N$, where $N = N(t)$ depends on time t. The dislocation at $i = 1$ is immobile and represents the source, as we discuss below. The dislocations for $i = 2, \ldots, N$ are mobile and have constant Burgers vector $b_i = b$. The Burgers vector is directed along x for edge dislocations and along z for screw ones.

To describe the dynamics of mobile dislocations we use an overdamped equation, so that the velocity of dislocations depends linearly on the resolved shear stress exerted on it [20]. The equation of motion for the mobile dislocations is given by

$$\chi \frac{dx_i}{dt} = b_i\left(\sigma + \sum_{\substack{j=1\\(j\neq i)}}^{N} \sigma_{i,j}^{\mathrm{int}} + \sigma_i^{\mathrm{img}}\right) + \sum_P f(x_i - X_P), \quad (1)$$

where χ is an effective viscosity and σ is the external stress. The interaction stress $\sigma_{i,j}^{\mathrm{int}}$ between dislocations i and j is computed taking into account the image stresses of dislocation j due to the open boundary conditions (a similar method is used in electrostatics), while σ_i^{img} is due to the interaction between dislocation i and its own images. A compact expression of the interaction and image stresses can be obtained by performing the sum over the images [21], yielding

$$\begin{aligned}\sigma_{i,j}^{\mathrm{int}} &= -\frac{\pi}{2L}\frac{\mu b_j}{k}\left[\cot\left(\pi\frac{x_j - x_i}{2L}\right) + \cot\left(\pi\frac{x_j + x_i}{2L}\right)\right],\\ \sigma_i^{\mathrm{img}} &= -\frac{\pi}{2L}\frac{\mu b_i}{k}\cot\left(\pi\frac{x_i}{L}\right),\end{aligned} \quad (2)$$

where μ is the shear modulus, $k = \pi$ for screw dislocations and $k = 2\pi(1 - \nu)$ for edge dislocations, and ν is the Poisson ratio. We notice here that the sum over the images is exact only in the case of screw dislocations. For edge dislocations, there is an additional subdominant correction scaling as $1/r^2$ that we neglect here since it should not influence the scaling behavior. The last term in Eq. (1) represents the interactions with pinning centers placed at randomly chosen positions X_P with $P = 1, \ldots, N_P$. The detailed shape $f(x)$ of the individual pinning force is inessential for most purposes, provided it is of short-range nature, and in this case it is given by

$$f(x) = -f_0 \frac{x}{\xi_P} e^{-(x/\xi_P)^2}, \quad (3)$$

where ξ_P is the range of the interaction and f_0 controls its strength.

Dislocations are typically generated by Frank-Read-like sources, which can only be represented in a three dimensional model. In lower dimensions, it is customary to model the source phenomenologically by creating dislocations with a certain rate. The drawback of this approach is that the new dislocation produces an artificial discontinuity in the stress field. To overcome this problem, we employ a method suggested by Zaiser [22] in which a source is represented by an immobile dislocation, placed at position x_1, with a time-dependent Burgers vector $b_1(t)$ growing with stress. When $b_1(t) = b$, a new mobile dislocation is emitted from the source whose Burgers vector is reset to zero. The evolution equation for $b_1(t)$ is given by

$$\chi_1 \frac{db_1}{dt} = \theta(\sigma_1^{\mathrm{eff}})\sigma_1^{\mathrm{eff}}, \quad (4)$$

where θ is the Heaviside step function and χ_1 is a damping constant that we set equal to $\chi_1 = \chi/b$. The effective stress $\sigma_1^{\mathrm{eff}} = \sigma + \sigma_1^{\mathrm{int}} + \sigma_1^{\mathrm{img}}$ is the sum of the constant external stress σ, the stress σ_1^{int} produced by the interaction between the source and the mobile dislocations (including the relative images), and the stress σ_1^{img} produced by the interaction between the source and its own images. These stresses are obtained from Eq. (2) observing that $\sigma_1^{\mathrm{int}} = \sum_{j=2}^{N} \sigma_{i=1,j}^{\mathrm{int}}$ and $\sigma_1^{\mathrm{img}} = \sigma_{i=1}^{\mathrm{img}}$.

Integrating numerically Eqs. (1) and (4), we analyze the dynamics of the pileup as a function on the external stress σ and the system size L. The units of time, space, and forces are chosen so that $b = 1$, $\chi = 1$, and $\mu/k = 1$. For the simulations reported here, we considered parameters $L = 256$, 512, 1024, 2048, 4096, 8192, $x_1 = 16$, and the pinning centers are Poisson distributed with an average spacing $d_p = L/N_p = 2$ with $f_0 = 1$ and $\xi = 1$. The final steady-state is independent from the initial conditions that we have chosen to be a dislocation-free line, apart from the source. From the experimental point of view, a key quantity describing the growth of the slip line is the plastic strain rate $\dot{\epsilon}$ given by

$$\dot{\epsilon} \equiv \frac{1}{L}\sum_i b_i \dot{x}_i = b\rho v, \quad (5)$$

where $\rho = N/L$ is the dislocation density and $v = \sum \dot{x}_i/N$ is the average dislocation velocity. Notice that all these quantities are defined per unit dislocation length, given the effective one-dimensional geometry of our model.

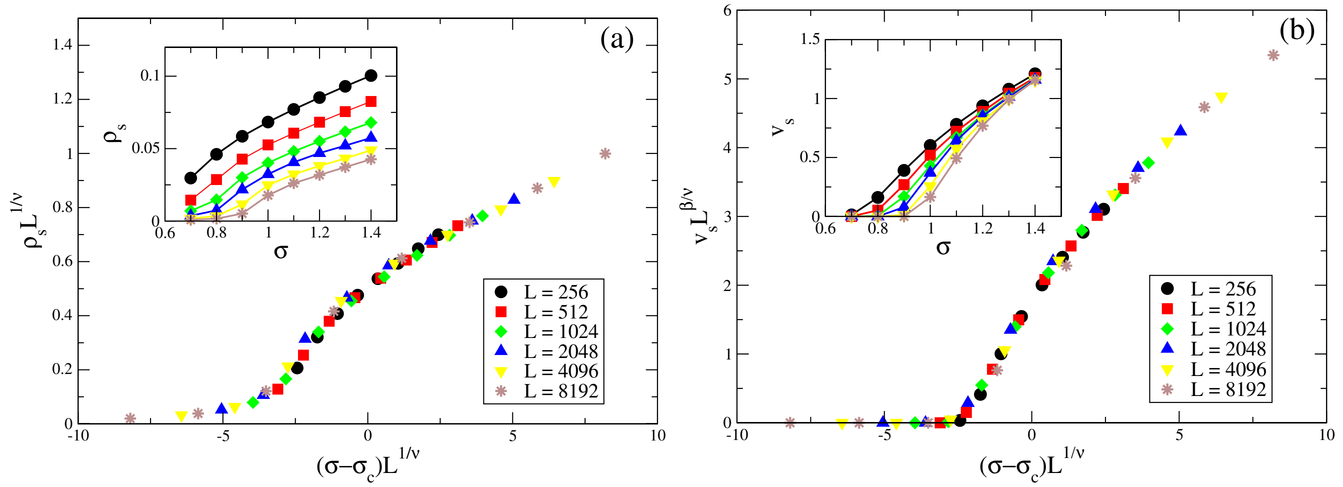

FIG. 2 (color online). (a) The average stationary density of the pileup as a function of the system size L for different values of the applied stress σ (inset). The data collapse is consistent with the scaling hypothesis in Eq. (6) with the exponents $\alpha = 1.00 \pm 0.02$ and $1/\nu = 0.35 \pm 0.02$. (b) The average stationary velocity of the pileup as a function of the system size L for different values of the applied stress σ (inset). The data collapse is consistent with the scaling hypothesis in Eq. (6) with the exponents $\beta = 0.48 \pm 0.02$ and $\nu = 2.85 \pm 0.05$.

Since the strain rate is simply the product of the dislocation density and average velocity, we study directly these two quantities. We find that after an initial transient the density and the velocity reach a steady-state value (ρ_s and v_s, respectively) that depends on the system size L and the applied stress σ as shown in the insets of Fig. 2. The graphs are suggestive of a nonequilibrium phase transition controlled by the stress between a pinned phase at low stress and a moving phase at large stresses. The curves become sharper close to the depinning point as L is increased, as expected when finite-size effects are present. To confirm this idea we perform a scaling collapse according to

$$\begin{aligned} \rho_s(\sigma, L) &= L^{-\alpha/\nu} f[(\sigma - \sigma_c)L^{1/\nu}], \\ v_s(\sigma, L) &= L^{-\beta/\nu} g[(\sigma - \sigma_c)L^{1/\nu}], \end{aligned} \tag{6}$$

where the scaling function $f(u)$ satisfies the limits

$$f(u) \simeq \begin{cases} 1 & \text{if } u \ll 1 \\ u^{\alpha} & \text{if } u \gg 1, \end{cases} \tag{7}$$

and for $g(u)$ they are

$$g(u) \simeq \begin{cases} 1 & \text{if } u \ll 1 \\ u^{\beta} & \text{if } u \gg 1. \end{cases} \tag{8}$$

The best collapse is obtained using $\sigma_c = 1.05 \pm 0.05$, $\nu = 2.85 \pm 0.05$, $\alpha/\nu = 0.35 \pm 0.02$, and $\beta/\nu = 0.17 \pm 0.02$, as shown in Fig. 2. These exponent combinations correspond to $\alpha = 1.00 \pm 0.02$, $\beta = 0.48 \pm 0.02$, and yield a scaling form for the strain rate of the type

$$\dot{\epsilon}(\sigma, L) = L^{-(\alpha+\beta)/\nu} h[(\sigma - \sigma_c)L^{1/\nu}], \tag{9}$$

where $h(u) = f(u)g(u)$, as we have also verified directly.

We have also analyzed the slip line growth dynamics in the transient regime. The time dependence of the dislocation density and velocity can also be characterized by finite-size scaling functions which at the critical point $\sigma = \sigma_c$ are given by

$$\rho(t, L) = L^{-\alpha/\nu} f_t[t/L^z], \qquad v(t, L) = L^{-\beta/\nu} g_t[t/L^z], \tag{10}$$

where z is the dynamic exponent. The best collapse is obtained for $z = 1.25 \pm 0.02$, as shown in Fig. 3. The scaling functions, for small values of the argument, scale as $f_t(u) \sim u^{\zeta}$, with $\zeta = 0.55 \pm 0.05$, and $g_t(u) \sim u^{-\theta}$, with $\theta = 0.10 \pm 0.05$. Hence, the strain rate in the initial phase grows as $\dot{\epsilon}(t) \sim t^{\zeta-\theta}$. Notice that the scaling expo-

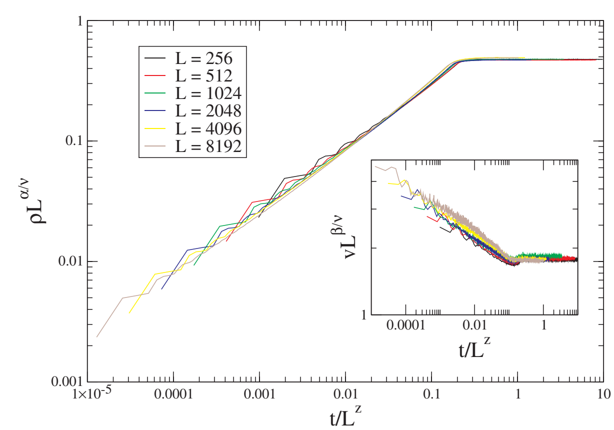

FIG. 3 (color online). The evolution of the dislocation density and velocity (inset) as a function of the system size L at the critical point $\sigma = \sigma_c = 1.05$. The best collapse is obtained for $\alpha/\nu = 0.35 \pm 0.02$, $\beta/\nu = 0.17 \pm 0.02$, and $z = 1.25 \pm 0.02$, which is consistent with the scaling collapse in Fig. 2.

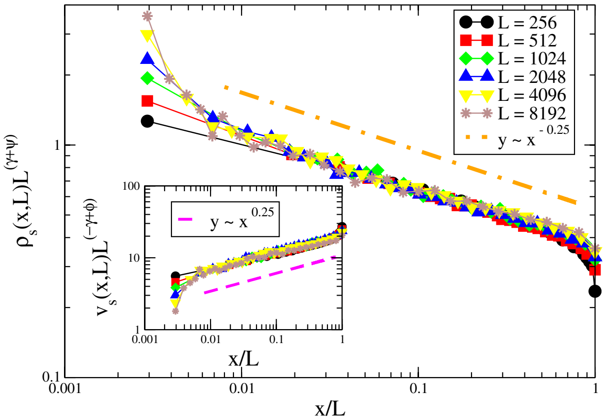

FIG. 4 (color online). The density $\rho_s(x, L)$ and velocity $v_s(x, L)$ (inset) profile for different values of the system size L, for $\sigma = 1.05$ (critical regime). In the bulk of the line we have the power-law behavior $\rho_s(x, L) \sim x^{-\gamma}/L^{\psi}$ and $v_s(x, L) \sim x^{\gamma}/L^{\phi}$ with $\gamma = 0.25 \pm 0.02$, $\psi = 0.09 \pm 0.02$, and $\phi = 0.42 \pm 0.02$. These behaviors are consistent with the scaling of the stationary density and velocity in the critical regime.

nents are considerably different from what is expected for a regularly spaced pileup with periodic boundary conditions, where the density is constant (hence $\alpha = 0$) and the critical exponents are $\beta \simeq 0.78$, $z \simeq 0.78$, and $\nu \simeq 1.5$ [19].

To elucidate the role of the boundary condition and characterize the internal morphology of the pileup, we report in Fig. 4 the stationary density $\rho_s(x, L)$ and velocity $v_s(x, L)$ profiles for different values of the system size L, for $\sigma = \sigma_c = 1.05$. We observe inhomogeneities for both density and velocity profiles which can be described as power laws: $\rho_s(x, L) \sim x^{-\gamma}/L^{\psi}$ and $v_s(x, L) \sim x^{\gamma}/L^{\phi}$, with $\gamma \simeq 0.25 \pm 0.02$, $\psi \simeq 0.09 \pm 0.02$, and $\phi = 0.42 \pm 0.02$. Notice that the strain-rate profile is approximately constant since the two power laws cancel out in the product. This result could have been expected since in the steady state the average dislocation flux should be constant [i.e., $\partial\rho/\partial t = -\nabla(v\rho) = 0$]. The scaling of the profiles is also consistent with the scaling of the stationary density and velocity as described in Eq. (6). In particular, we have that

$$\rho_s(\sigma_c, L) = \frac{1}{L}\int_{x_1}^{L} \rho_s(x, L)dx \sim L^{-(\gamma+\psi)}. \tag{11}$$

Hence, we have the scaling relation $\gamma + \psi = \alpha/\nu$ that is verified by the numerical values of the exponents. Similarly, from the steady-state velocity equation

$$v_s(\sigma_c, L) = \frac{\int_{x_1}^{L} \rho_s(x, L)v_s(x, L)dx}{\int_{x_1}^{L} \rho_s(x, L)dx} \sim L^{-(\phi-\gamma)} \tag{12}$$

we obtain the relation $\phi - \gamma = \beta/\nu$, which is again in agreement with our numerical estimates. Notice that the scaling laws above only apply at the critical point $\sigma = \sigma_c$. For $\sigma < \sigma_c$, the profiles do not span the entire system size, defining a penetration length $\lambda_p < L$.

In conclusion, we have studied the slip line formation at the initial stage of plastic deformation in a crystal by means of the double-ended pileup model and found that in the presence of pinning centers (quenched disorder) the model exhibits a nonequilibrium phase transition. As a consequence of this dislocation density, velocity and strain rate are described by finite-size scaling. Finite-size scaling has direct implications for size effects: the size dependence of the yield stress σ_Y observed in micron-scale plasticity [2]. Considering the scaling law in Eq. (6), we expect that the yield stress for finite L grows towards the asymptotic value σ_c according to $\sigma_Y(L) = \sigma_c - A/L^{1/\nu}$, where A is a positive constant. This type of inverse size effect, with the strength increasing with the sample size, is due to the larger back stress exerted on the source by the pileup as its length is increased. In more general cases, involving many sources and several slip lines, the constant A is expected to be negative as shown in other models of the yielding transition [1].

This work is supported by the European Commission's NEST Pathfinder program TRIGS under Contract No. NEST-2005-PATH-COM-043386. We thank M. Zaiser for useful discussions.

[1] M. Zaiser, Adv. Phys. **55**, 185 (2006).
[2] M. D. Uchic *et al.*, Science **305**, 986 (2004).
[3] D. M. Dimiduk *et al.*, Science **312**, 1188 (2006).
[4] F. F. Csikor *et al.*, Science **318**, 251 (2007).
[5] J. Weiss and J. R. Grasso, J. Phys. Chem. B **101**, 6113 (1997).
[6] M.-C. Miguel *et al.*, Nature (London) **410**, 667 (2001).
[7] R. F. Tinder and J. P. Trzil, Acta Metall. **21**, 975 (1973).
[8] H. H. Pothoff, Phys. Status Solidi A **77**, 215 (1983).
[9] H. Godon, H. H. Potoff, and H. Neuhäuser, Cryst. Res. Technol. **19**, 373 (1984).
[10] A. J. Liu and S. R. Nagel, Nature (London) **396**, 21 (1998).
[11] M. Kardar, Phys. Rep. **301**, 85 (1998).
[12] F. R. N. Nabarro, Proc. R. Soc. A **381**, 285 (1982).
[13] S. Zapperi and M. Zaiser, Mater. Sci. Eng., A **309–310**, 348 (2001).
[14] M.-C. Miguel *et al.*, Phys. Rev. Lett. **89**, 165501 (2002).
[15] M. Zaiser and P. Moretti, J. Stat. Mech. (2005) P08004.
[16] H. Neuhäuser, in *Dislocations in Solids*, edited by F. R. N. Nabarro (North-Holland, Amsterdam, 1983), Vol. 6.
[17] H. Neuhäuser, O. B. Arkan, and H. Flor, Czechoslovak Journal of Physics, Section B **38**, 511 (1988).
[18] O. B. Arkan and H. Neuhäuser, Phys. Status Solidi A **99**, 385 (1987).
[19] P. Moretti *et al.*, Phys. Rev. B **69**, 214103 (2004).
[20] M. F. Kanninen and A. R. Rosenfield, Philos. Mag. **20**, 569 (1969).
[21] J. P. Hirth and J. Lothe, *Theory of Dislocations* (Wiley and Sons, New York, 1984).
[22] M. Zaiser (private communication).